International Journal of Robotics and Control Systems
Vol. 5, No. 2, 2025, pp. 830-845
ISSN 2775-2658
http://pubs2.ascee.org/index.php/ijrcs

Optimized Selective Harmonic Elimination in CHB-MLI Using Red-Tailed Hawk Algorithm for Unequal DC Sources

Elaf Hamzah Yahia [a,1], Hasan Salman Hamad [b,2,*], Shouket A. Ahmed [c,3,*], Taha Abdulsalam Almalaisi [d,4], Hasan S. Majdi [e,5], Omer K. Ahmed [d,6], Nitin Solke [f,7], Ravi Sekhar [f,8]

[a] Electrical Engineering Department, Engineering College, University of Anbar, Iraq
[b] Technical College of Engineering, Al-Bayan University, Baghdad, Iraq
[c] Department of Medical Instrumentation Techniques Engineering, Technical Engineering College, Al-Kitab University, Altun Kupri, Kirkuk, Iraq
[d] Renewable Energies Researches Unit, Northern Technical University, Kirkuk, Iraq
[e] Department of Chemical Engineering and Petroleum Industries, Al-Mustaqbal University College, 51001 Hillah, Babylon, Iraq
[f] Symbiosis Institute of Technology (SIT) Pune Campus, Symbiosis International (Deemed University) (SIU), Pune, 412115, Maharashtra, India
[1] elaf.yahia@uoanbar.edu.iq; [2] hasan.s@albayan.edu.iq; [3] shouketunimap@gmail.com; [4] almalaisipi@gmail.com;
[5] dr.hasanshker@mustaqbal.edu.iq; [6] omerkalil@yahoo.com; [7] nitin.solke@sitpune.edu.in; [8] ravi.sekhar@sitpune.edu.in
* Corresponding Author

ARTICLE INFO

Article history
Received January 16, 2025
Revised February 18, 2025
Accepted February 25, 2025

Keywords
Selective Harmonic Elimination (SHE);
Cascaded H-Bridge Multilevel Inverter (CHB-MLI);
Red-Tailed Hawk Algorithm (RTHA);
Total Harmonic Distortion (THD);
Renewable Energy

ABSTRACT

The study develops an optimized SHE procedure to regulate a CHB-MLI powered by PV modules which use unequal DC sources. The main goal involves finding suitable switching angles that produce minimal low-order harmonics during steady output voltage operation under variable input scenarios. The Red-Tailed Hawk Algorithm (RTHA) serves as a recent bio-inspired metaheuristic optimization method to solve effectively the nonlinear transcendental SHE equations. The MATLAB/Simulink environment implements a validation of the proposed method by modeling a three-phase 7-level CHB-MLI system. A performance evaluation of the proposed algorithm occurs against established optimization methods consisting of Particle Swarm Optimization (PSO) and Grey Wolf Optimization (GWO) and Whale Optimization Algorithm (WOA). Total Harmonic Distortion reduction, computational efficiency and convergence rate serve as the three main performance indicators for evaluation. The experimental findings show RTHA accomplishes higher harmonic reduction while offering improved speed and stability when dealing with unequal DC voltage issues when contrasted against traditional optimization methods. RTHA operates better than analytical approaches in real-world inverter applications through its flexible and adaptable approach despite needing complex calculations and preset conditions. The scale-up of RTHA applications requires additional research because excessive computational requirements and initial value dependencies must be addressed. The research shows that RTHA-based SHE optimization represents a viable and implementable solution for power quality advancement in renewable energy systems.

1. Introduction

Selectively eliminating harmonics using SHE technology has become an essential breakthrough in power electronics that solves primary power system harmonic distortion issues [1]-[5]. The design concept behind Multi-Level Inverters (MLIs) involves multiple voltage synthesis levels to produce high-quality outputs which reduces machine efficiencies and system reliability through lower harmonic interference. The ability of MLIs to reduce harmonic distortions leads to decreased power losses as well as decreased electromagnetic interference and enhanced operation in both industrial power systems and grid-connected applications [6]-[8]. Excessive losses in copper windings become a severe power quality problem alongside skin effect deterioration and unwanted torque pulsations of electric machines and excessive heater intensity of the neutral conductor [9]-[11]. These problems arise from harmonic distortions caused by nonlinear loads, switching devices and system imbalances. Harmonic distortions degrade the functional efficiency of transformers generators and motors so effective harmonic suppression methods must be implemented. SHE represents an optimal solution because it enables harmonics of certain orders to be eliminated while maintaining control over the fundamental component which enhances system performance and stability [12]-[15].

Studies on SHE-based techniques have progressed substantially but their application to multi-level inverters remains complex because of the demanding requirement to solve difficult nonlinear transcendental equations that establish switching angles. Numerical techniques together with iterative methods and metaheuristic optimization algorithms exist to discover optimal switching angles for harmonic elimination. The approaches demonstrate good results yet struggle from multiple drawbacks which include problems reaching local optima and high complexity levels and sensitivity to initial starting points [16]-[18]. The research focuses on using the Red-Tailed Hawk Algorithm (RTHA) from reference [19] to find solutions for SHE equations that operate Cascaded H-Bridge Multi-Level Inverters (CHB MLIs) driven by photovoltaic (PV) panels. The main advantage of using RTHA for switching angle optimization comes from its capability to achieve optimal results without requiring additional harmonic filtering mechanisms. RTHA surpasses standard algorithms like PSO and GWO and WOA since it delivers rapid convergence besides strong resistance under changing conditions and exceptional harmonic suppression abilities [20]-[22].

R. H. Park introduced SHE in 1976 and the strategy underwent extensive improvements to become an essential component for PWM voltage-source converters [19]. The solution methods for solving SHE equations present a significant problem which becomes worse in cases involving DC input voltage fluctuation such as PV-integrated power systems [23]. The research demonstrates a more efficient and processor-friendly method for SHE problem resolution through RTHA proof which maintains optimal harmonic eradication across changing operational conditions [24]-[29].

The main points of this research contribution consist of:

1. The paper evaluates multi-level inverter SHE techniques and outlines the problems with finding optimal switching angle solutions.
2. The Red-Tailed Hawk Algorithm (RTHA) serves as a method for solving SHE equations in CHB MLI systems which makes the system less dependent on additional harmonic filtering technologies.
3. Comparative performance analysis of RTHA against other metaheuristic algorithms (PSO, GWO, WOA) in terms of convergence speed, accuracy, and robustness.
4. Simulation results validate that RTHA successfully minimizes harmonics without compromising the power quality nor efficiency when used in PV-powered CHB MLI.

This paper follows a structured format that includes details about related research along with SHE optimization methods in Section 2. Section 3 describes the mathematical formulation of SHE equations and the implementation of RTHA. The Section 4 presents simulation findings and displays performance evaluations. This work demonstrates its conclusions in Section 5 alongside a discussion of possible advancements for optimization-based harmonic elimination techniques.

2. Cascaded H-bridge Inverters

The circuit diagram of the 7-level three-phase cascaded H-bridge multilevel inverter (CHB-MLI) appears in Fig. 1. A series connection of multiple H-bridge modules enables this inverter to operate through separate independent discrete DC sources. Fig. 1 of the paper shows both the correspondent output waveform and the single-phase configuration for CHB-MLI systems [30]-[36]. The output voltage level count for CHB-MLI systems follows the calculation L=2n+1which depends on the independent DC source quantity. A seven-level CHB-MLI needs three H-bridge modules which receive power from different DC sources for proper output voltage waveform generation.

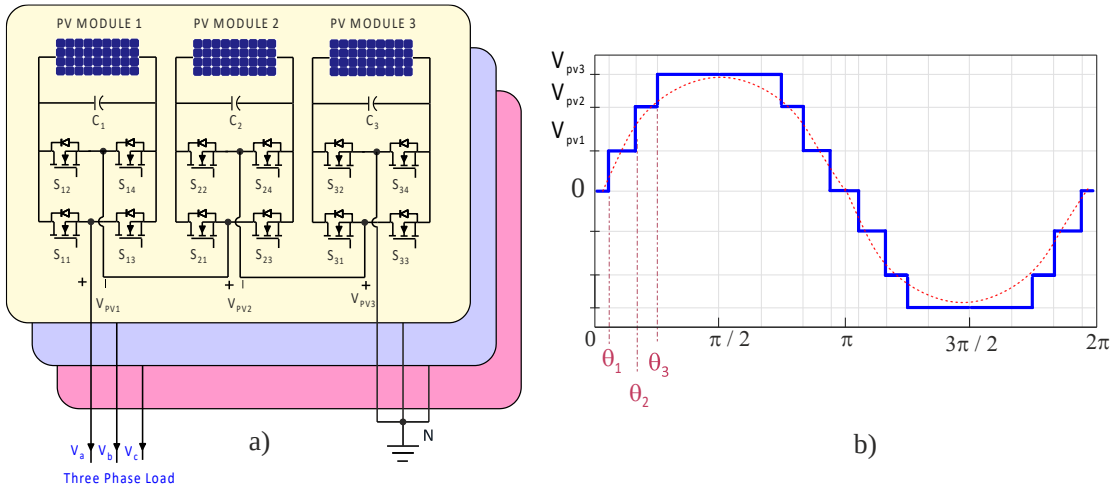

Fig. 1. Three-phase 7-level CHB-MLI: (a) Circuit diagram (b) Single-phase output voltage waveform [19]

3. Challenges of Selective Harmonic Elimination in MLI

In the SHE equations, the switching angles at the fundamental frequency are achieved by solving the equations in such a way that the fundamental voltage is obtained in the desired manner and the undesired or chosen lower order harmonics are removed. It is necessary to perform a single switching operation for every module that is part of a loop in order to minimize switching losses and improve electromagnetic interference (EMI) [37]-[41]. As a result, the number of switching angles is equivalent to the number of separate DC sources, denoted by the letter n. Due to the fact that k represents the number of switches, it is possible to remove n-1 low-order harmonics from the output voltage of the inverter machine. The nonlinear harmonic equations that are necessary to attain optimum switching angles in 7-level CHB-MLI may be explained by providing an explanation using the Fourier expansion of the output voltage. The expression of the output voltage, which takes into account all of the harmonic components, may be stated as (1).

$$V_{ab}(\omega t) = \sum_{(odd)n=1,3,\ldots}^{\infty} \frac{4}{\pi n}[V_{PV1}\cos(n\theta_1) + V_{PV2}\cos(n\theta_2) + V_{PV3}\cos(n\theta_3)]\sin(\omega t) \quad (1)$$

where VPV1, VPV2, and VPV3 are input the PV panel voltage. The elements θ1, θ2, and θ3 represent the switching angles, and they are required to fulfill the constraint that $0 < \theta1 < \theta2 < \theta3 < \pi/2$. The third harmonic component along with its multiples do not affect phase-to-phase voltages in balanced three-phase systems. The elimination of harmonic orders from the line voltage waveform must be done before switching at the low frequency. These harmonic orders include the fifth, seventh, eleventh, and so on. In the event that the equations are rearranged in the following manner:

$$\begin{aligned} V_{\text{fund}} &= V_{\text{PV1}}\cos(\theta_1) + V_{\text{PV2}}\cos(\theta_2) + V_{\text{PV3}}\cos(\theta_3) \\ V_{5^{th}} &= V_{\text{PV1}}\cos(5\theta_1) + V_{\text{PV2}}\cos(5\theta_2) + V_{\text{PV3}}\cos(5\theta_3) \\ V_{7^{th}} &= V_{\text{PV1}}\cos(7\theta_1) + V_{\text{PV2}}\cos(7\theta_2) + V_{\text{PV3}}\cos(7\theta_3) \end{aligned} \quad (2)$$

Shows (2) how the first SHE equation controls basic waveform amplitude. Setting other equations to zero eliminates specified harmonics. An appropriate approach solves these equations. Keeping the voltage at the fundamental frequency and minimizing low-order harmonics (V5, V7, etc.) is the goal. This work presents RTHA optimization to get the optimum SHE equation solutions. THD may be determined using (3) in three-phase systems. THDe is computed up to the 7th harmonic using the same procedure.

$$THD = \frac{\sqrt{V_5^2 + V_7^2 + V_{11}^2 + \cdots}}{|V_1|} \tag{3}$$

The fitness function used for SHE-PWM is defined as follows: Each term must be equal to zero (4) and (5).

$$f = \min_{\theta_i} \left\{ \left| V_{fund} - V_{ref} \right| + \left(\left| V_{5^{th}} \right|^2 + \left| V_{7^{th}} \right|^2 \right) \right\} = 0 \tag{4}$$

$$V_{fund} - V_{ref} \leq \varepsilon \tag{5}$$

In this research, Vref represents the intended reference voltage, ε denotes the permissible error tolerance, with ε set at 1 V as the acceptable answer. The first term governs the fundamental voltage, whereas the subsequent term denotes low-order harmonics within the fitness function.

4. Red-Tailed Hawk Algorithm (RTHA)

In this algorithm, the hunting behavior of the red-tailed hawk is simulated to provide an optimal solution for complex problems in constrained search spaces. In hunting, red-tailed hawks perform strategies such as monitoring, flanking, and soaring. The proposed Red-Tailed Hawk Algorithm (RTHA) follows this hunting behavior using new terminologies like flapper and soar M, as well as possessing monitoring behaviors. RTHA is initially applied to solve the combined economic and environmental dispatch problem, and its algorithm performances are investigated by comparing its results with previously developed optimization algorithms [42]-[48]. The effect of changing the relevant operational parameters on the effectiveness of the RTHA is also scrutinized. The innovative algorithm is then applied to solve the harmonic elimination problem in the cascaded H-bridge multilevel inverter and investigations are conducted into the RTHA inspired selective harmonic elimination problem to obtain an effective solution [20].

RTHA, inspired by the hunting behavior of the red-tailed hawk, involves a set of homogeneous durables performing some basic strategies. In the simulation, a bird population with some active members having similar searching capabilities performs monitoring strategies. Additionally, some well-performing but non-active members enable monitoring behavior. While moving, the red-tailed hawks' route approaches the monitoring path. To alleviate the "curse of dimensionality," soar M is introduced for seeking campaigns, and different roles known as flappers and soarers are owned by the hunting network [49]-[54]. An efficient hunting network consists of some active birds referred to as flappers that search for food by moving randomly around between the stopping and staring points. When searching around the prey, the waiting chance of the flapper birds is determined by their success rate. Birds with high success separation between the flanking location and the prey endure watching. After the praying prey is detected, a soar M behavior directs the flapping birds to go to the prey one. Birds can perform either the monitoring, flapper, or both strategies depending on their success rates and their ability to obtain a better solution.

During high soaring Fig. 2 (a): the bird flies at a high altitude with its wings in a slight dihedral, flapping as little as possible in order to save energy and investigate the region that has been chosen. Low soaring Fig. 2 (b): after the target location has been chosen, the red-tailed fly will perform a low soaring maneuver in a spiral movement around the prey. With the help of this movement, it is able to

determine the optimal place and timing to strike the target. Stooping and swooping Fig. 2 (c): after picking the optimal position and moment in the previous stage, the red-tailed swooped its prey by stooping and increasing its acceleration (from 32-64 to 190 kilometers per hour) in a curved trajectory.

a) High Soaring b) Low Soaring c) Stopping& Swooping

Fig. 2. Behavior of red-tailed hawk during hunting [16]

4.1. Mathematical Model

The red-tailed hawk (RTH) algorithm that has been proposed is designed to imitate the RTH's hunting behavior. The acts that are carried out throughout each step of the search are outlined and represented. The high soaring, low soaring, and stooping and swooping phases are the three stages that are included in this algorithm.

4.1.1. High Soaring

The red-tailed hawk will fly to great heights in the sky in order to locate the most advantageous place in terms of the availability of food. The way in which red-tailed hawks behave at the high soaring stage is seen in Fig. 3, and the mathematical model of this stage is represented by (6):

$$X(t) = X_{best} + (X_{mean} - X(t-1)).Levy(dim).TF(t) \quad (6)$$

whereas X(t) denotes the location of the red-tailed hawk at the iteration t, Xbest denotes the position that was attained with the greatest success, and Xmean is the mean of the positions. The levy flight distribution function, which can be computed using (7), is denoted by the symbol levy, while the transition factor function, which can be calculated using (8), is denoted by the symbol TF(t).

$$Levy(dim) = s\frac{\mu.\sigma}{|\upsilon|^{\beta-1}} \quad (7)$$

$$\sigma = \left(\frac{\Gamma(1+\beta).sin(\pi\beta/2)}{\Gamma(1+\beta/2).\beta.2^{(1-\beta/2)}}\right) \quad (8)$$

where s is a constant that is equal to 0.01; dim is the dimension of the issue; β is a constant that is equal to 1.5; υ and σ are random values that where T_{max} represents the max number of iterations (9).

$$TF(t) = 1 + sin(2.5 + (\frac{t}{T_{max}}) \quad (9)$$

4.1.2. Low Soaring

Through a technique known as low soaring, the hawk encircles its prey by flying in a spiral pattern that is considerably closer to the ground. This stage is shown in Fig. 4, and its model may be represented in the following manner (10) and (11):

$$X(t) = X_{best} + (x(t) + y(t).StepSize(t) \quad (10)$$

$$StepSize(t) = X(t) - X_{mean} \tag{11}$$

while x and y represent the direction coordinates, which may be computed using the following formula (12):

$$\begin{cases} x(t) = R(t) \cdot \sin(\theta(t)) \\ y(t) = R(t) \cdot \cos(\theta(t)) \end{cases} \begin{cases} R(t) = R_0 \cdot (r - t/T_{\max}) \cdot \text{ rand} \\ \theta(t) = A \cdot (1 - t/T_{\max}) \cdot \text{ rand} \end{cases} \begin{cases} x(t) = x(t)/max\,|x(t)| \\ y(t) = y(t)/max\,|y(t)| \end{cases} \tag{12}$$

where R0 is the beginning value of the radius, which ranges from 0.5 to 3, A is the angel gain, which ranges from 5 to 15, rand is a random gain, which ranges from 0 to 1, and r is a control gain, which ranges from 1 to 2. According to the explanation provided in Fig. 5, these factors allow the hawk to fly around the prey in a spiraling motion.

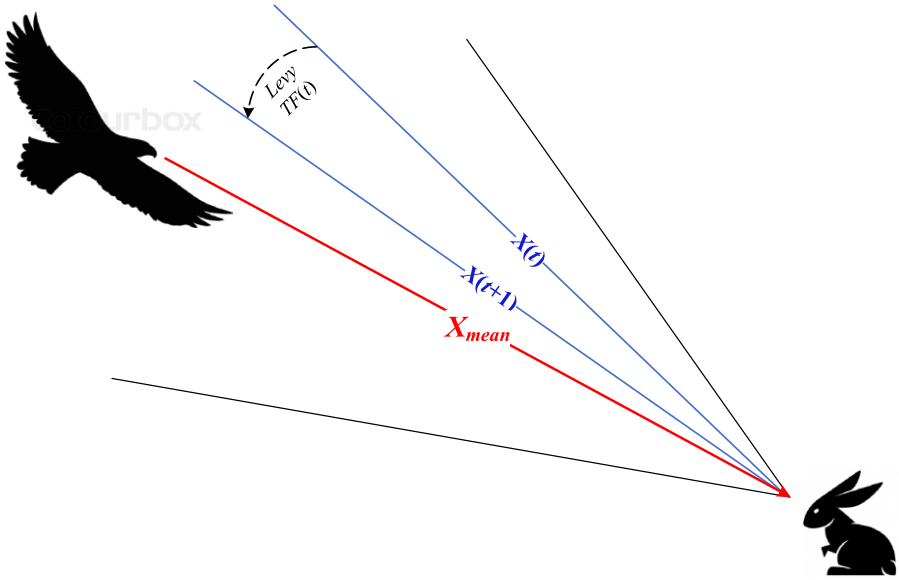

Fig. 3. Behavior of red-tailed hawk during high soaring stage [16]

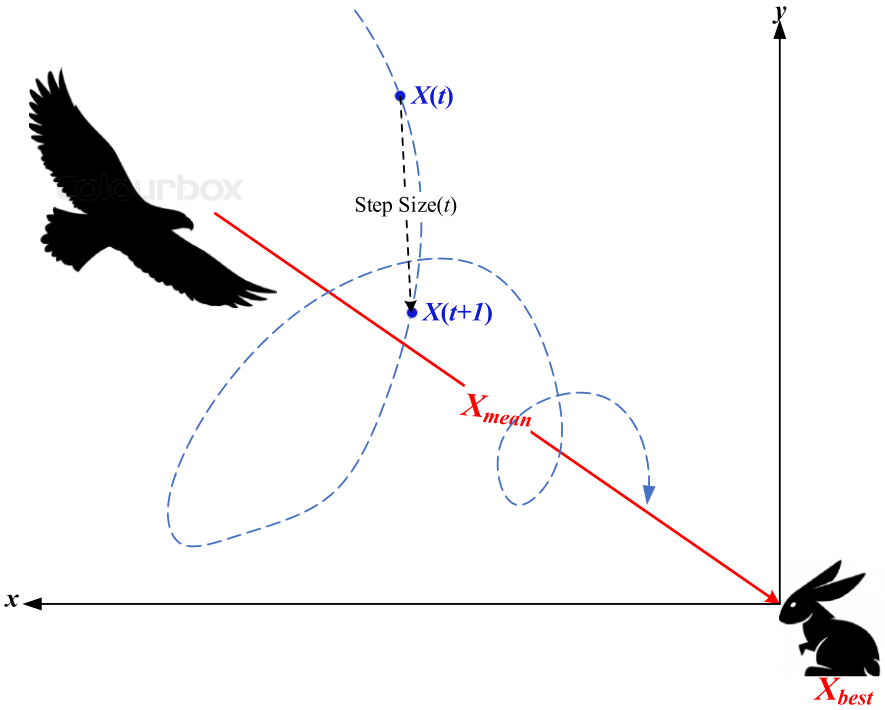

Fig. 4. Behavior of red-tailed hawk during low soaring stage [16]

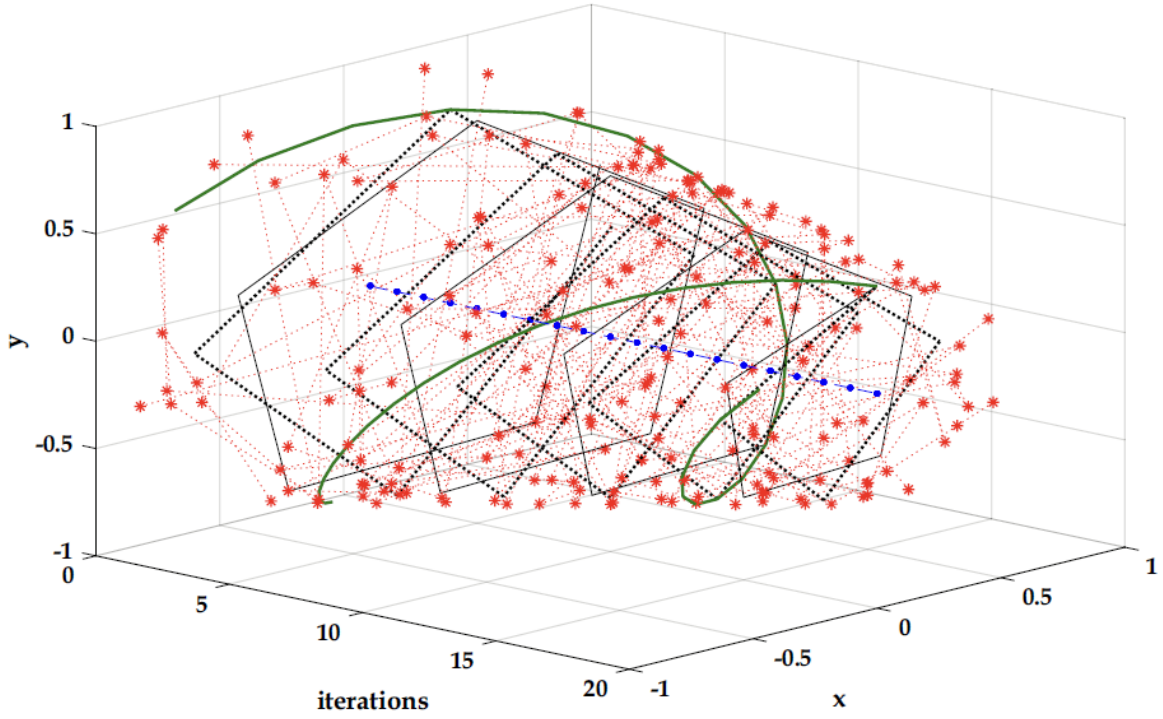

Fig. 5. Evolution of the direction coordinates as a function of iterations [16]

4.1.3. Stooping and Swooping

The hawk rapidly drops to the ground and launches an assault on the prey from the position that it has secured the most advantageously during the low flying stage. The behavior of the red-tailed hawks at this period is shown in Fig. 3, according to the author. Modeling this step may be done in the following way (13):

$$X(t) = \alpha(t) \cdot X_{\text{best}} + x(t) \cdot StepSize1(t) + y(t) \cdot StepSize2(t) \tag{13}$$

And the following formula may be used to compute each step size (14):

$$\begin{aligned} StepSize1(t) &= X(t) - TF(t) \cdot X_{\text{mean}} \\ StepSize2(t) &= G(t) \cdot X(t) - TF(t) \cdot X_{\text{best}} \end{aligned} \tag{14}$$

Considering the acceleration and gravity components, denoted by α and G, respectively, it is possible to define them in the following manner (15):

$$\begin{aligned} \alpha(t) &= \sin^2\left(2.5 - t / T_{\max}\right) \\ G(t) &= 2 \cdot \left(1 - t / T_{\max}\right) \end{aligned} \tag{15}$$

The acceleration of the hawk, shown by α, rises as t increases, which improves the convergence speed. The gravity effect, denoted by G, diminishes, which reduces the exploitation diversity, as the hawk gets closer to its prey. See Fig. 6 for an explanation of this stage. The pseudo code of the algorithm is given in Table 1. The parameters of the algorithm for the SHE PWM problem are given in Table 2.

5. Simulation Results

To determine the optimal switching angles, the RTHA optimization method is implemented as an m-file in MATLAB. The cascaded H-bridge multilevel inverter (CHB-MLI) is subsequently

configured based on the computed switching angles. In this study, multiple combinations are generated by randomly varying the input voltages within the range of 50 to 60 V, with a resolution of 1 V. The corresponding input voltages and the calculated switching angles using, PSO, GWO, WOA, and RTHA are presented in Table 3, Table 4, Table 5, and Table 6, respectively.

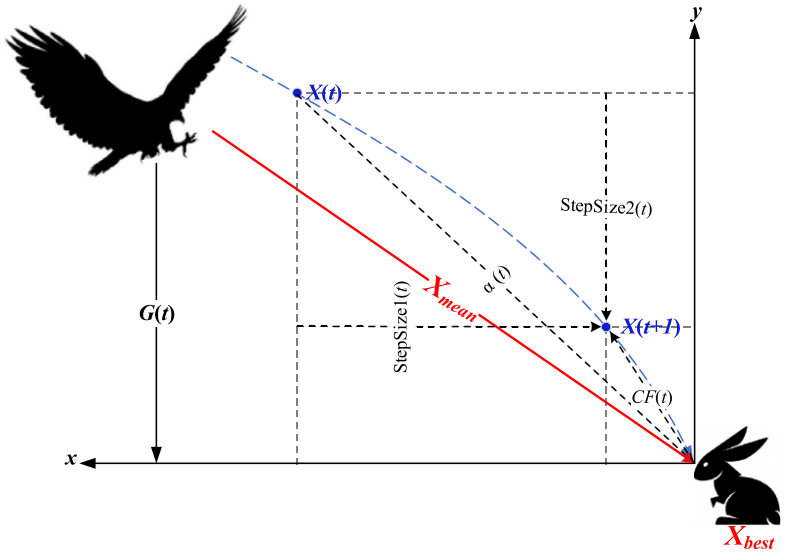

Fig. 6. Behavior of red-tailed hawk during stooping and swooping stages [16]

Table 1. RTH pseudocode [16]

Initialize population randomly within the search space.
While t < Tmax do:
  High Soaring Stage:
    For each individual i in population (Npop):
      Compute Lévy flight distribution (8).
      Calculate transition factor TF (9).
      Update position using (6).
    End for
    Low Soaring Stage:
    For each individual i in population (Npop):
      Compute direction coordinates (12).
      Update position using (10).
    End for
    Stooping and Swooping Stage:
    For each individual i in population (Npop):
      Compute acceleration and gravity factors (15).
      Calculate step size (14).
      Update position using (13).
    End for
End while

Table 2. The RTH parameters [16]

Parameters	Value	Parameters	Value
Number of variables	3	A	15
Iteration number	100	R_0	0.5
Number of the population	30	r	1.5

Fig. 7 illustrates the convergence rates of PSO, GWO, WOA, and RTH algorithms for Case 10, with (a) showing the overall performance in a semilogy plot and (b) providing a zoomed-in view for detailed comparison. As shown in Fig. 7 (b), the RTH algorithm converged within the 8th iteration, whereas PSO, GWO, and WOA achieved convergence at the 24th, 32nd, and 40th iterations, respectively. For the tenth case, with input voltages (VPV1 = 54V, VPV2 = 50 V, and VPV3 = 53 V),

the switching angles calculated using all algorithms were applied to the inverter. The corresponding simulation results for this case are shown in Fig. 8, Fig. 9, Fig. 10, Fig. 11, respectively.

Table 3. Angles obtained with PSO

PSO - SHE										
no	**V_1**	**V_2**	**V_3**	**θ_1**	**θ_2**	**θ_3**	**V1p(rms)**	**error (%)**	**THD (%)**	**THDe (%)**
1	50	50	53	0.209	0.492	0.997	109.3	0.70%	7.99	0.21
2	50	52	51	0.193	0.508	1.007	109.3	0.70%	8.19	0.26
3	50	53	57	0.210	0.564	1.056	109.3	0.70%	7.28	1.16
4	50	55	52	0.195	0.553	1.050	109.3	0.70%	7.60	0.87
5	50	58	51	0.193	0.589	1.071	109.3	0.70%	7.98	0.51
6	50	59	52	0.205	0.614	1.079	109.3	0.70%	8.10	0.23
7	51	52	56	0.207	0.563	1.050	109.3	0.70%	7.10	0.98
8	51	57	50	0.199	0.583	1.066	109.3	0.70%	7.67	0.64
9	53	59	53	0.244	0.676	1.095	109.3	0.70%	9.18	0.67
10	54	50	53	0.209	0.555	1.049	109.3	0.70%	7.07	1.32

Table 4. Angles obtained with GWO

GWO -SHE										
no	**V_1**	**V_2**	**V_3**	**θ_1**	**θ_2**	**θ_3**	**V1p(rms)**	**error (%)**	**THD (%)**	**THDe (%)**
1	50	50	53	0.213	0.492	0.993	109.5	0.50%	7.83	0.14
2	50	52	51	0.196	0.509	1.003	109.5	0.50%	8.18	0.03
3	50	53	57	0.219	0.579	1.042	109.5	0.50%	6.58	0.21
4	50	55	52	0.193	0.563	1.040	109.5	0.50%	7.30	0.12
5	50	58	51	0.191	0.592	1.067	109.4	0.60%	7.82	0.28
6	50	59	52	0.199	0.610	1.076	109.6	0.40%	7.99	0.09
7	51	52	56	0.214	0.569	1.040	109.5	0.50%	6.73	0.16
8	51	57	50	0.188	0.585	1.062	109.5	0.50%	7.68	0.43
9	53	59	53	0.240	0.669	1.098	109.5	0.50%	9.17	0.33
10	54	50	53	0.221	0.578	1.033	109.3	0.70%	6.50	0.22

Table 5. Angles obtained with WOA

WOA -SHE										
no	**V_1**	**V_2**	**V_3**	**θ_1**	**θ_2**	**θ_3**	**V1p(rms)**	**error (%)**	**THD (%)**	**THDe (%)**
1	50	50	53	0.207	0.495	0.996	109.3	0.70%	7.92	0.10
2	50	52	51	0.196	0.501	1.002	109.3	0.70%	8.02	0.19
3	50	53	57	0.215	0.573	1.042	109.7	0.30%	6.71	0.10
4	50	55	52	0.195	0.560	1.037	109.7	0.30%	7.36	0.05
5	50	58	51	0.192	0.587	1.064	109.7	0.30%	7.71	0.25
6	50	59	52	0.200	0.612	1.073	109.7	0.30%	7.81	0.21
7	51	52	56	0.218	0.571	1.035	109.7	0.30%	6.68	0.17
8	51	57	50	0.197	0.588	1.054	109.7	0.30%	7.24	0.21
9	53	59	53	0.230	0.659	1.104	109.6	0.40%	9.17	0.28
10	54	50	53	0.220	0.563	1.033	109.7	0.30%	6.70	0.27

Table 6. Angles obtained with RTH

RTH -SHE										
no	**V_1**	**V_2**	**V_3**	**θ_1**	**θ_2**	**θ_3**	**V1p(rms)**	**error (%)**	**THD (%)**	**THDe (%)**
1	50	50	53	0.2080	0.4798	0.9863	110.00	0.00%	**7.74**	**0.04**
2	50	52	51	0.1965	0.4977	0.9963	110.00	0.00%	**8.01**	**0.02**
3	50	53	57	0.2126	0.5676	1.0382	110.00	0.00%	**6.86**	**0.05**
4	50	55	52	0.1935	0.5529	1.0331	110.00	0.00%	**7.56**	**0.03**
5	50	58	51	0.1912	0.5844	1.0575	110.00	0.00%	**7.50**	**0.02**
6	50	59	52	0.1980	0.6041	1.0709	110.00	0.00%	**7.82**	**0.04**
7	51	52	56	0.2137	0.5626	1.0336	110.00	0.00%	**6.90**	**0.06**
8	51	57	50	0.1926	0.5802	1.0529	110.00	0.00%	**7.33**	**0.02**
9	53	59	53	0.2311	0.6570	1.0972	110.00	0.00%	**8.98**	**0.04**
10	54	50	53	0.2167	0.5605	1.0275	110.00	0.00%	**6.90**	**0.05**

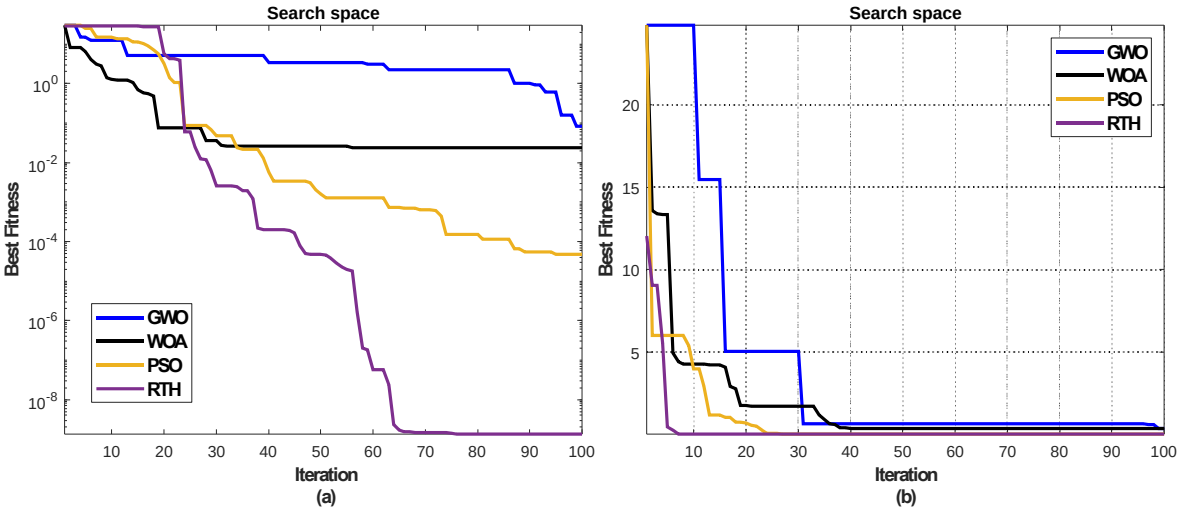

Fig. 7. Convergence Rates of Optimization Algorithms (PSO, GWO, WOA, and RTH) for Case 10. (a) Full Convergence Trend (semilogy), (b) Focused View (Zoomed-in)"

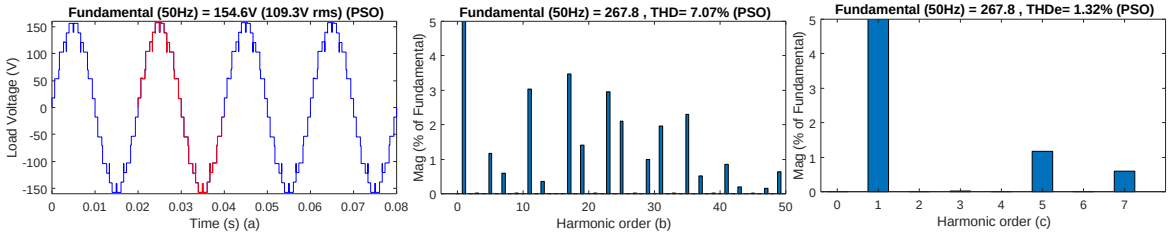

Fig. 8. For case 10 (PSO), a) output voltage waveform b) THD result (line to line) c) THDe result (line to line)

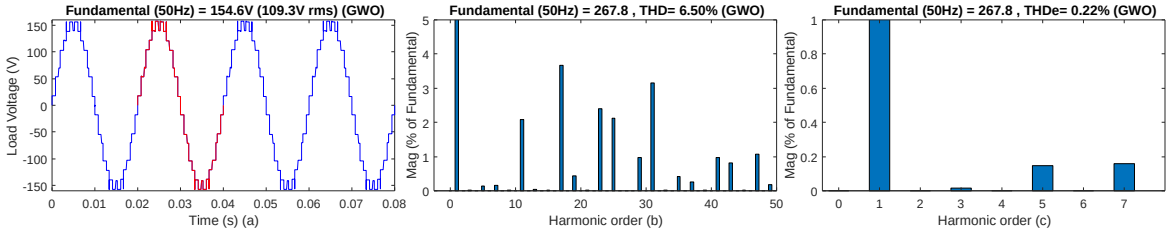

Fig. 9. For case 10 (GWO), a) output voltage waveform b) THD result (line to line) c) THDe result (line to line)

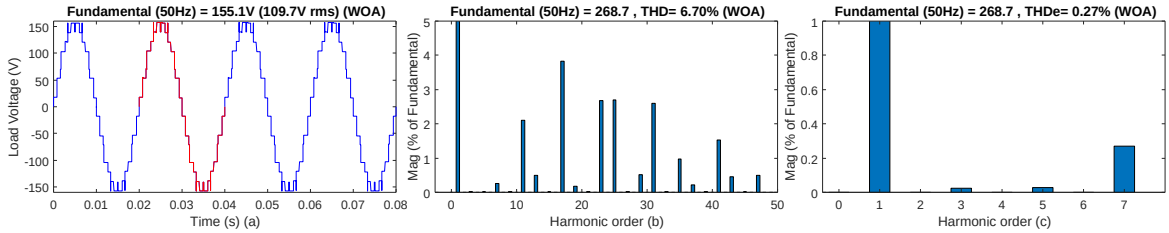

Fig. 10. For case 10 (WOA), a) output voltage waveform b) THD result (line to line) c) THDe result (line to line)

- **PSO** demonstrates moderate performance, achieving a fundamental voltage of 154.6 V peak (109.3 V rms), with a relatively higher THD (7.07%) and THDe (1.32%). Fig. 8.
- **GWO** outperforms PSO by reducing THD to 6.50% and THDe to 0.22%, while maintaining the same fundamental voltage of 154.6 V peak (109.3 V rms). Fig. 9.

- **WOA** slightly improves upon GWO, yielding a higher fundamental voltage of 155.1 V peak (109.7 V rms) and comparable THD (6.70%) and THDe (0.22%). Fig. 10.
- **RTHA** demonstrates the best performance among all algorithms, achieving the highest fundamental voltage of 155.6 V peak (110.0 V rms) and effectively minimizing THDe to 0.05%, with a competitive THD of 6.90%. Fig. 11.

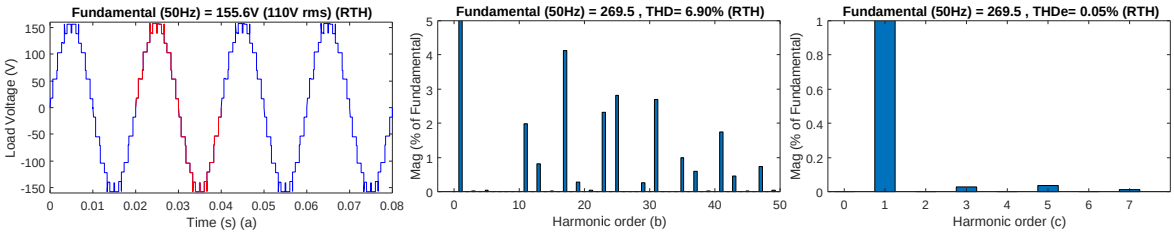

Fig. 11. For case 10 (RTH), a) output voltage waveform b) THD result (line to line) c) THDe result (line to line)

These results indicate that RTHA is the most effective algorithm for reducing harmonics and maintaining high-quality output voltage, followed by WOA and GWO, with PSO exhibiting relatively lower performance. In a three-phase seven-level cascaded H-bridge multilevel inverter (CHB-MLI), the tables include the outcomes of four optimization algorithms: PSO, GWO, WOA, and RTH, all of which were used for selective harmonic elimination (SHE). The findings demonstrate that regardless of the input voltage changes, the fundamental voltage stays within the range of 109.3 V to 110.0 V rms across all algorithms. This means that all methods successfully maintain the intended output value. The algorithms all have very low error percentages; however, RTH achieves zero error, indicating that it offers the most accurate solution when contrasted with PSO, GWO, and WOA, which all show slightly larger but still low error numbers. Though acceptable, PSO's Total Harmonic Distortion (THD) readings of 7.07% to 9.18% are somewhat more than the other algorithms. While there is significant fluctuation, GWO generally performs better, with THD values between 6.50% and 9.17%. In comparison to PSO and GWO, WOA produces THD values ranging from 6.68 to 7.92%, suggesting superior harmonic suppression. With THD levels below 8% in every test instance and a continuous range of 6.73–7.82%, RTH clearly demonstrates its excellent harmonic reduction capabilities. As a last point, the Total Harmonic Distortion error (THDe) readings for PSO vary from 0.21% to 1.32%, indicating a certain amount of harmonic inaccuracy. GWO decreases this dispersion, with THDe values between 0.03% and 0.33%. While WOA's THDe values range from 0.05% to 0.28%, they are still marginally more than GWO's. Among these methods, RTH stands out as the most effective in reducing harmonic errors, with THDe values between 0.02% and 0.06%.

6. Conclusions

RTHA delivered higher performance results than PSO and GWO and WOA since it excelled at minimizing THD and THDe. RTHA produced Total Harmonic Distortion results between 6.73% and 7.82% and Total Harmonic Distortion error results down to 0.02% which verifies its robust ability to minimize harmonic distortion effectively. The algorithm proved its excellence in performance by demonstrating harmonic distortion reduction that outshined its competitors thus establishing itself as an optimal choice for harmonic optimization in multilevel inverters. RTHA shows two primary advantages through its accurate operation and stable performance. All test results demonstrated complete accuracy because RTHA proved to be the exclusive algorithm capable of generating zero errors while maintaining the desired output voltage. The performance of this algorithm stood out from other methods because its output voltage reached the exact specifications without any errors while competing algorithms produced minor inaccuracies. RTHA delivers precise voltage control which qualifies it as an optimal optimization technique when systems need detailed voltage level regulation such as renewable energy-based multilevel inverters.

RTHA's performance included more accurate results alongside faster run times along with superior efficiency than the other methods PSO, GWO, and WOA. RTHA proved perfect for real-time operations in multilevel inverter systems since it delivered fast and efficient optimization solutions for switching angles and stable operational stability. The RTHA method converges to optimal solutions in quicker time spans which makes it advantageous in restricted computational situations especially during time-critical processes. The harmonic distortion levels from RTHA performance exceed those of alternative algorithms because of its exceptional ability to ensure clean inverter output. The algorithm generated lower harmonic distortion that surpassed PSO and GWO and WOA values thus proving its strength for effective harmonic suppression across all harmonic orders. RTHA demonstrates its suitability as an optimal technological solution for high-quality output demands because PV systems and renewable energy integration require knowledge about harmonic distortion reduction for maximum system performance.

The wide range of operational capabilities along with applicability define RTHA as a powerful tool. The algorithm operates in different multilevel inverter systems because its design fits various inverter topologies and operational conditions. RTHA provides adaptable functionality to support varied input voltage conditions which maintains regular harmonic reduction and output voltage equilibrium in real life operations. RTA provides high practical value for applications in renewable energy systems because it ensures superior output quality in PV-powered multilevel inverters when input voltage fluctuations occur. The RTHA needs more comprehensive research that extends its examination to different inverter types and operating conditions. Studies need to study how RTHA functions when operating in less-than-optimal conditions that impact both its stability and operational efficiency. The evaluation of RTHA through testing under different modulation methods and system conditions would confirm its potential for use in diverse operational situations. The planned adaptations will maintain RTHA's suitability toward increasing requirements of flexible and scalable power system operations. RTHA stands as an exceptionally dependable optimization method for Multilevel inverter She which demonstrates better performance than PSO, GWO, WOA and alternative evolutionary techniques. RTHA demonstrates superior capability in reducing THD and THDe alongside accurate performance and quick convergence time while providing versatility which positions it as an outstanding optimization method for renewable energy systems including photovoltaic systems and power electronics. Additional investigations about SHE performance under various operating conditions, different inverter topologies, and system configurations must be conducted to both verify its optimal functionality as well as discover enhanced possibilities for harmonic reduction and efficiency improvement and real-time system optimization.

Author Contribution: All authors contributed equally to the main contributor to this paper. All authors read and approved the final paper.

Acknowledgment: Hasan Salman Hamad expresses his appreciation to Al-Bayan University which has offered the equipment and the opportunities that enable this study by Al-Bayan University, Technical College of Engineering, Baghdad – 10011, Iraq.

Conflicts of Interest: The authors declare no conflict of interest.

References

[1] M. S. A. Dahidah, G. Konstantinou and V. G. Agelidis, "A Review of Multilevel Selective Harmonic Elimination PWM: Formulations, Solving Algorithms, Implementation and Applications," *IEEE Transactions on Power Electronics*, vol. 30, no. 8, pp. 4091-4106, 2015, https://doi.org/10.1109/TPEL.2014.2355226.

[2] M. Ali, F. S. Al-Ismail, M. M. Gulzar, M. Khalid, "A review on harmonic elimination and mitigation techniques in power converter based systems," *Electric Power Systems Research*, vol. 234, p. 110573, 2024, https://doi.org/10.1016/j.epsr.2024.110573.

[3] S. Choudhury, M. Bajaj, T. Dash, S. Kamel, F. Jurado, "Multilevel inverter: A survey on classical and advanced topologies, control schemes, applications to power system and future prospects," *Energies*, vol. 14, no. 18, p. 5773, 2021, https://doi.org/10.3390/en14185773.

[4] H. Naderi, N. Ghaderi, M. Abedini, "Improving power quality and efficiency of multi-level inverter system through intelligent control algorithm," *Soft Computing*, pp. 1-14, 2024, https://doi.org/10.1007/s00500-024-10354-5.

[5] S. Munawar, M. S. Iqbal, M. Adnan, M. Ali Akbar and A. Bermak, "Multilevel Inverters Design, Topologies, and Applications: Research Issues, Current, and Future Directions," *IEEE Access*, vol. 12, pp. 149320-149350, 2024, https://doi.org/10.1109/ACCESS.2024.3472752.

[6] N. S. Tuhin, Y. Arafat, "Design and Performance Analysis of a Novel Asymmetrical Multilevel Inverter Structure With Reduced Components Using the Half-Height Modulation Technique," *International Transactions on Electrical Energy Systems*, vol. 2025, no. 1, pp. 1-21, 2025, https://doi.org/10.1155/etep/5546944.

[7] S. D. Biswas, B. Das, C. Nandi, "A comprehensive review of optimization techniques for power quality improvement using multilevel inverters," *AIP Conference Proceedings*, vol. 3242, no. 1, p. 050004, 2024, https://doi.org/10.1063/5.0234302.

[8] A. Sivapriya, N. Kalaiarasi, "A Review on Cascaded H-Bridge and Modular Multilevel Converter: Topologies, Modulation Technique and Comparative Analysis," *Advanced Power Electronics Converters for Future Renewable Energy Systems*, pp. 195-222, 2023, https://doi.org/10.1201/9781003323471-9.

[9] C. Buccella, C. Cecati, M. G. Cimoroni and K. Razi, "Harmonic mitigation technique for multilevel inverters in power systems," *2014 International Symposium on Power Electronics, Electrical Drives, Automation and Motion*, pp. 73-77, 2014, https://doi.org/10.1109/SPEEDAM.2014.6872070.

[10] S. N L and S. G, "Hybrid Multilevel Inverter Control for Harmonic Mitigation," *2023 International Conference on Control, Communication and Computing (ICCC)*, pp. 1-6, 2023, https://doi.org/10.1109/ICCC57789.2023.10165006.

[11] T. Karmakar, S. D. Biswas, S. Bhattacharjee, C. Nandi, B. Das, "Harmonic mitigation in multilevel inverters for power quality improvement in power system," *AIP Conference Proceedings*, vol. 3242, no. 1, p. 050002, 2024, https://doi.org/10.1063/5.0234391.

[12] M. A. Hannan, Z. A. Ghani, M. M. Hoque, P. J. Ker, A. Hussain and A. Mohamed, "Fuzzy Logic Inverter Controller in Photovoltaic Applications: Issues and Recommendations," *IEEE Access*, vol. 7, pp. 24934-24955, 2019, https://doi.org/10.1109/ACCESS.2019.2899610.

[13] A. Benevieri, S. Cosso, A. Formentini, M. Marchesoni, M. Passalacqua, L. Vaccaro, "Advances and Perspectives in Multilevel Converters: A Comprehensive Review," *Electronics*, vol. 13, no. 23, p. 4736, 2024, https://doi.org/10.3390/electronics13234736.

[14] S. A. Abed, "Big Data and Artificial Intelligence on the Blockchain: A Review," *Babylonian Journal of Artificial Intelligence*, vol. 2023, 1-4, 2023, https://doi.org/10.58496/BJAI/2023/001.

[15] G. Amirthayogam, N. Kumaran, S. Gopalakrishnan, K. A. Brito, S. RaviChand, S. B. Choubey, "Integrating behavioral analytics and intrusion detection systems to protect critical infrastructure and smart cities," *Babylonian Journal of Networking*, vol. 2024, pp. 88-97, 2024, https://doi.org/10.58496/BJN/2024/010.

[16] S. Ferahtia *et al.*, "Red-tailed hawk algorithm for numerical optimization and real-world problems," *Scientific Reports*, vol. 13, no. 1, p. 12950, 2023, https://doi.org/10.1038/s41598-023-38778-3.

[17] Y. Gopal, K. P. Panda, D. Birla, M. Lalwani, "Swarm Optimization-Based Modified Selective Harmonic Elimination PWM Technique Application in Symmetrical H-Bridge Type Multilevel Inverters," *Engineering, Technology & Applied Science Research*, vol. 9, no. 1, pp. 3836-3845, 2019, https://doi.org/10.48084/etasr.2397.

[18] F. Chabni, R. Taleb, A. Lakhedar, M. Bounadja, "New modified CHB multilevel inverter topology with elimination of lower and higher order harmonics," *Automatika*, vol. 59, no. 1, pp. 1-10, 2018, https://doi.org/10.1080/00051144.2018.1484549.

[19] Y. Bektaş, H. Karaca, "Red deer algorithm based selective harmonic elimination for renewable energy application with unequal DC sources," *Energy Reports*, vol. 8, pp. 588-596, 2022, https://doi.org/10.1016/j.egyr.2022.05.209.

[20] L. Chen, N. Song, Y. Ma, "Harris hawks optimization based on global cross-variation and tent mapping," *The Journal of Supercomputing*, vol. 79, no. 5, pp. 5576-5614, 2023, https://doi.org/10.1007/s11227-022-04869-7.

[21] B. Sharma, S. Manna, V. Saxena, P. K. Raghuvanshi, M. H. Alsharif, M. K. Kim, "A comprehensive review of multi-level inverters, modulation, and control for grid-interfaced solar PV systems," *Scientific reports*, vol. 15, no. 1, p. 661, 2025, https://doi.org/10.1038/s41598-024-84296-1.

[22] A. M. Abdel-Hamed, A. M. Nasser, H. Shatla, A. Refky, "An improved SPWM control approach with aid of ant lion optimization for minimizing the THD in multilevel inverters," *Scientific Reports*, vol. 15, no. 1, p. 1990, 2025, https://doi.org/10.1038/s41598-024-84678-5.

[23] S. Y. Mohammed, M. Aljanabi, "From Text to Threat Detection: The Power of NLP in Cybersecurity," *SHIFRA*, pp. 1-7, 2024, https://doi.org/10.70470/SHIFRA/2024/001.

[24] S. Y. Mohammed, A. K. Oleiwi, T. K. Asman, H. M. Saleh, A. M. Mahmood, I. Avci, "A Survey of MCDM-Based Software Engineering Method," *Babylonian Journal of Mathematics*, vol. 2023, pp. 13-18, 2024, https://doi.org/10.58496/BJM/2024/002.

[25] M. Aljanabi, "Safeguarding connected health: Leveraging trustworthy AI techniques to harden intrusion detection systems against data poisoning threats in IoMT environments," *Babylonian Journal of Internet of Things*, vol. 2023, pp. 31-37, 2023, https://doi.org/10.58496/BJIoT/2023/005.

[26] A. Singh, V. Jately, P. Kala, Y. Yang, "Enhancing power quality in electric vehicles and battery energy storage systems using multilevel inverter topologies–A review," *Journal of Energy Storage*, vol. 110, p. 115274, 2025, https://doi.org/10.1016/j.est.2024.115274.

[27] A. K. Bhardwaj, P. K. Dutta, P. Chintale, "AI-Powered Anomaly Detection for Kubernetes Security: A Systematic Approach to Identifying Threats," *Babylonian Journal of Machine Learning*, vol. 2024, pp. 142-148, 2024, https://doi.org/10.58496/BJML/2024/014.

[28] M. M. Shwaysh, S. Alani, M. A. Saad, T. A. Abdulhussein, "Image Encryption and Steganography Method Based on AES Algorithm and Secret Sharing Algorithm," *Ingenierie des Systemes d'Information*, vol. 29, no. 2, pp. 705-714, 2024, https://doi.org/10.18280/isi.290232.

[29] M. S. Hossain *et al*., "Performance evaluation of a nearest level control-based TCHB multilevel inverter for PMSM motors in electric vehicle systems," *Results in Engineering*, vol. 25, p. 103949, 2025, https://doi.org/10.1016/j.rineng.2025.103949.

[30] M. Al-Mukhtar, A. A. Abbas, A. H. Hamad, M. H. Al-hashimi, "Normalized-UNet Segmentation for COVID-19 Utilizing an Encoder-Decoder Connection Layer Block," *Journal of Image and Graphics*, vol. 12, no. 1, pp. 66-75, 2024, https://doi.org/10.1016/j.rineng.2025.103949.

[31] X. Zheng *et al*., "Topology Construction, Modeling, and Control of Multi-level Inverters without shoot-through problem," *IEEE Transactions on Power Electronics*, pp. 1-14, 2025, https://doi.org/10.1109/TPEL.2025.3532675.

[32] A. H. Hamad, A. A. Mahmood, S. A. Abed, X. Ying, "Semantic relatedness maximisation for word sense disambiguation using a hybrid firefly algorithm," *Journal of Intelligent & Fuzzy Systems*, vol. 41, no. 6, pp. 7047-7061, 2021, https://doi.org/10.3233/JIFS-210934.

[33] S. Q. Salih *et al*., "Enhanced Total Harmonic Distortion Optimization in Cascaded H-Bridge Multilevel Inverters Using the Dwarf Mongoose Optimization Algorithm," *Journal of Robotics and Control*, vol. 5, no. 6, pp. 1862-1871, 2024, https://doi.org/10.18196/jrc.v5i6.23548.

[34] V. Ramanarayana, K. N. Rao, B. Kumar, S. V. K. Naresh, "A single-phase five-level multilevel inverter with rated power fault-tolerant feature," *AEU-International Journal of Electronics and Communications*, vol. 190, p. 155645, 2025, https://doi.org/10.1016/j.aeue.2024.155645.

[35] X. Ying, A. H. Hamad, "A hybrid bat algorithm based on combined semantic measures for word sense disambiguation," *Advances in Natural Computation, Fuzzy Systems and Knowledge Discovery*, pp. 149–157, 2019, https://doi.org/10.1007/978-3-030-32456-8_16.

[36] T. A. Taha *et al*., "Enhancing Multilevel Inverter Performance: A Novel Dung Beetle Optimizer-based Selective Harmonic Elimination Approach," *Journal of Robotics and Control (JRC)*, vol. 5, no. 4, pp. 944-953, 2024, https://doi.org/10.18196/jrc.v5i4.21722.

[37] T. A. Taha, N. I. A. Wahab, M. K. Hassan, H. I. Zaynal, F. H. Taha, A. M. Hashim, "Real-Time Optimal Switching Angle Scheme for a Cascaded H-Bridge Inverter using Bonobo Optimizer," *Journal of Robotics and Control (JRC)*, vol. 5, no. 4, pp. 918-930, 2024, https://doi.org/10.18196/jrc.v5i4.21701.

[38] H. Juma'a, T. Atyia, "Design and Implementation of multi-level inverter for PV system with various DC Sources," *NTU Journal of Renewable Energy*, vol. 5, no. 1, pp. 24-33, 2023, https://doi.org/10.56286/ntujre.v5i1.554.

[39] H. Mansourizadeh, M. Hosseinpour, A. Seifi, M. Shahparasti, "A 13-level switched-capacitor-based multilevel inverter with reduced components and inrush current limitation," *Scientific Reports*, vol. 15, no. 1, p. 290, 2025, https://doi.org/10.1038/s41598-024-84148-y.

[40] Z. Ali, Z. M. Abdullah, B. A. Naser, R. W. Daoud, A. H. Ahmed, "Design of a Single-Phase Inverter for Solar Energy Conversion System," *NTU Journal of Renewable Energy*, vol. 1, no. 1, pp. 38-42, 2021, https://doi.org/10.56286/ntujre.v1i1.13.

[41] E. H. I. Albajari, S. R. Aslan, "Exploring the Synergy of Integration: Assessing the Performance of Hydraulic Storage and Solar Power Integration in Kirkuk city," *NTU Journal of Renewable Energy*, vol. 5, no. 1, pp. 1-7, 2023, https://doi.org/10.56286/ntujre.v5i1.525.

[42] E. Bektaş *et al*., "Enhancing Harmonic Reduction in Multilevel Inverters using the Weevil Damage Optimization Algorithm," *Journal of Robotics and Control (JRC)*, vol. 5, no. 3, pp. 717-722, 2024, https://doi.org/10.18196/jrc.v5i3.21544.

[43] A. S. T. Hussain, D. Z. Ghafoor, S. A. Ahmed, T. A. Taha, "Smart inverter for low power application based hybrid power system," *AIP Conference Proceedings*, vol. 2787, no. 1, p. 050022, 2023, https://doi.org/10.1063/5.0150294.

[44] Z. Sarwer, M. N. Anwar, A. Sarwar, "Single phase switched-capacitor multilevel inverter with quadruple boosting and low voltage stress for renewable energy applications," *International Journal of Modelling and Simulation*, pp. 1-11, 2025, https://doi.org/10.1080/02286203.2024.2448338.

[45] T. A. Taha, M. K. Hassan, N. I. Abdul Wahab and H. I. Zaynal, "Red Deer Algorithm-Based Optimal Total Harmonic Distortion Minimization for Multilevel Inverters," *2023 IEEE IAS Global Conference on Renewable Energy and Hydrogen Technologies (GlobConHT)*, pp. 1-8, 2023, https://doi.org/10.1109/GlobConHT56829.2023.10087687.

[46] T. A. Taha, N. I. A. Wahab, M. K. Hassan, H. I. Zaynal, "Selective Harmonic Elimination in Multilevel Inverters Using the Bonobo Optimization Algorithm," *International Conference on Forthcoming Networks and Sustainability in the AIoT Era*, pp. 304-321, 2024, https://doi.org/10.1007/978-3-031-62871-9_24.

[47] R. Barzegarkhoo, M. Forouzesh, S. S. Lee, F. Blaabjerg and Y. P. Siwakoti, "Switched-Capacitor Multilevel Inverters: A Comprehensive Review," *IEEE Transactions on Power Electronics*, vol. 37, no. 9, pp. 11209-11243, 2022, https://doi.org/10.1109/TPEL.2022.3164508.

[48] S. Q. Salih, A. A. Alsewari, B. Al-Khateeb, M. F. Zolkipli, "Novel multi-swarm approach for balancing exploration and exploitation in particle swarm optimization," *Recent Trends in Data Science and Soft* Computing, pp. 196-206, 2019, https://doi.org/10.1007/978-3-319-99007-1_19.

[49] S. A. M. Al-Juboori, F. Hazzaa, Z. S. Jabbar, S. Salih, H. M. Gheni, "Man-in-the-middle and denial of service attacks detection using machine learning algorithms," *Bulletin of Electrical Engineering and Informatics*, vol. 12, no. 1, pp. 418-426, 2023, https://doi.org/10.11591/eei.v12i1.4555.

[50] S. Khazaeefar, M. Valizadeh, A. K. Sarvenoee, "An improved Z-source multi-level inverter scheme for grid-connected photovoltaic systems," *Electrical Engineering*, pp. 1-14, 2025, https://doi.org/10.1007/s00202-024-02943-2.

[51] T. Hai *et al*., "DependData: Data collection dependability through three-layer decision-making in BSNs for healthcare monitoring," *Information Fusion*, vol. 62, pp. 32-46, 2020, https://doi.org/10.1016/j.inffus.2020.03.004.

[52] V. P. Arumbu, D. Karthikeyan, "Reliability Assessment and Fault Prediction in a 13-Level Multilevel Inverter Through Machine Learning with SVM," *Journal of Electrical Engineering & Technology*, vol. 20, no. 1, pp. 473-488, 2025, https://doi.org/10.1007/s42835-024-01955-z.

[53] D. Dastan *et al*., "Insights into the photovoltaic properties of indium sulfide as an electron transport material in perovskite solar cells," *Scientific reports*, vol. 13, no. 1, p. 9076, 2023, https://doi.org/10.1038/s41598-023-36427-3.

[54] N. Karania, M. A. Alali, S. D. Gennaro, J. P. Barbot, "Hybrid control system for cascaded H-bridge multi-level inverter based shunt active filter for photovoltaic generation," *Electric Power Systems Research*, vol. 241, p. 111248, 2025, https://doi.org/10.1016/j.epsr.2024.111248.